Rat Tail Models for the Assessment of Injectable Nucleus Pulposus Regeneration Strategies

Marcos N. Barcellona[1,2] #, Emily E. McDonnell[1,2] #, Shani Samuel[1,2] and Conor T. Buckley[1,2,3,4*]

[1] Trinity Centre for Biomedical Engineering, Trinity Biomedical Sciences Institute, Trinity College Dublin, The University of Dublin, Dublin, Ireland

[2] Discipline of Mechanical, Manufacturing and Biomedical Engineering, School of Engineering, Trinity College Dublin, The University of Dublin, Dublin, Ireland

[3] Advanced Materials and Bioengineering Research (AMBER) Centre, Royal College of Surgeons in Ireland & Trinity College Dublin, The University of Dublin, Dublin Ireland

[4] Tissue Engineering Research Group, Department of Anatomy and Regenerative Medicine, Royal College of Surgeons in Ireland, 121/122 St. Stephen's Green Dublin 2, Ireland

# Both authors contributed equally to this article

*Corresponding author: Conor T. Buckley

E-mail address: conor.buckley@tcd.ie

Address: Trinity Centre for Biomedical Engineering, Trinity Biomedical Sciences Institute, Trinity College Dublin, Ireland

Telephone: +353-1-896-2061

Key words: Rat tail model; spine; puncture; degeneration, intervertebral disc, nucleus pulposus

Running Header: A systematic review and guide to rat tail models

ABSTRACT

Back pain is a global epidemiological and socioeconomic problem often associated with intervertebral disc degeneration; a condition believed to initiate in the nucleus pulposus (NP). There is considerable interest in developing early therapeutic interventions to target the NP and halt degeneration. Rat caudal models of disc degeneration have demonstrated significant utility in the study of disease progression and its impact on tissue structure, composition, and mechanical performance. One significant advantage of the caudal model is the ease of access and high throughput nature. However, considerable variability exists across the literature in terms of experimental setup and parameters. The objective of this article is to aid researchers in the design and development of caudal puncture models by providing details and insight into the most reported experimental parameters. Preferred Reporting Items for Systematic Reviews and Meta-Analyses (PRISMA) guidelines were employed to screen the existing literature and 80 manuscripts met the inclusion criteria. Disc geometry, surgical approaches, effect of needle gauge size to induce degeneration, therapeutic volume, outcome measures, and associated limitations are considered and discussed, and a range of recommendations based on different research questions are presented.

1 INTRODUCTION

Intervertebral disc (IVD) degeneration is an etiologically complex condition which remains one of the major contributors of disability at the global scale. The IVD is composed of three distinct compartments: the nucleus pulposus (NP), annulus fibrosus (AF), and cartilaginous endplates (CEPs). The AF is the outermost tissue responsible for resisting torsional stresses and providing structural stability to the disc.[1] It is largely composed of fibrillar collagens, which are aligned in concentric lamella oriented at approximately 120 degrees from their adjacent layers.[2-4] The CEPs border the disc on upper and lower planes and are composed of a thin layer of hyaline cartilage. The CEP is penetrated by a small vascular network which facilitates nutrient transport and gas exchange into and out of the disc.[5-7] The NP is the innermost compartment and is mostly responsible for the radial distribution of compressive stresses.[8, 9] When healthy, this tissue is a highly hydrated amorphous gelatinous matrix rich in proteoglycans and glycosaminoglycans, containing both fibrillar and nonfibrillar collagens, and smaller quantities of other proteins such as fibronectin and laminins.[8, 10-12] While changes have been observed throughout the whole motion segment as degeneration progresses,[13] degeneration is often believed to initiate within the NP, impairing the biomechanical function of the IVD. As a result, there is considerable research interest in early therapeutic interventions to target the NP and halt degeneration progressing outward through the AF.

Over the years a range of models have been developed to study the origins of disc degeneration, to further elucidate disease progression and to test innovative therapeutic strategies. When developing an in vivo animal model, multiple factors may affect the experimental outcome and need to be taken into careful consideration. Some of these factors include spine anatomy (shape/size), biomechanics as well as biochemical structure and species-specific pathophysiology.[14] During aging, the human IVD undergoes the rapid loss of notochordal cells. A similar phenomenon has been observed in goats, sheep, and chondrodystrophic dogs. However, pigs, rabbits, rats, and mice have been reported to retain a notochordal cell population into adulthood.[14-16] Furthermore, different species may be preferred or more suitable depending on the scientific question or objective of the study. For example, genetic

models in mice provide biologically relevant insight into factors that lead to degeneration such as sonic hedgehog signaling molecule knockout models, or aging-associated complications such as collagen and proteoglycan deficiencies.[17, 18] Alternatively, large animal models may be preferred for the clinical translation of regenerative therapeutics and implantable devices in discs of a more anatomically relevant scale comparable to the human IVD.[19, 20]

Rodent models, including both mouse and rat, offer significant advantages with regards to high throughput and ease of technology application.[15] While mouse models offer a wider range of genetic applications, rat models are often preferred when the objective is to deliver treatments locally into the intradiscal space. Within the scope of rat models, tail or caudal discs are of particular interest as they offer considerable advantages in terms of accessibility for surgical procedures, especially when repeated procedures are needed as is the case for surgically induced disc damage and treatment. The objective of this article is to aid researchers in the experimental setup and development of rat tail puncture models by providing details and insight into the most reported experimental parameters.

2 IDENTIFICATION OF PEER REVIEWED MANUSCRIPTS

Identification of the literature was conducted (initially in August 2021 and updated in March 2022) using the Preferred Reporting Items for Systematic Reviews and Meta-Analysis (PRISMA) guidelines set forth by Moher et al.[21] This comprehensive search was conducted in the databases PubMed, Scopus, and Medline using the search terms “intervertebral” AND “disc” AND “degeneration” AND “rat” AND (“needle puncture” OR “stab”). As highlighted in Figure **1**, this resulted in 146 unique manuscripts. The exclusion criteria included studies that were conducted using organ culture models, differing anatomical models (i.e., lumbar, cervical, or sacral discs), conference abstracts, articles in non-English languages, review papers, and nonrelated outputs (i.e., sand rat models or other nonrelevant animal models). After applying these exclusion criteria, a total of 80 manuscripts were retained for review (Table **S1**).

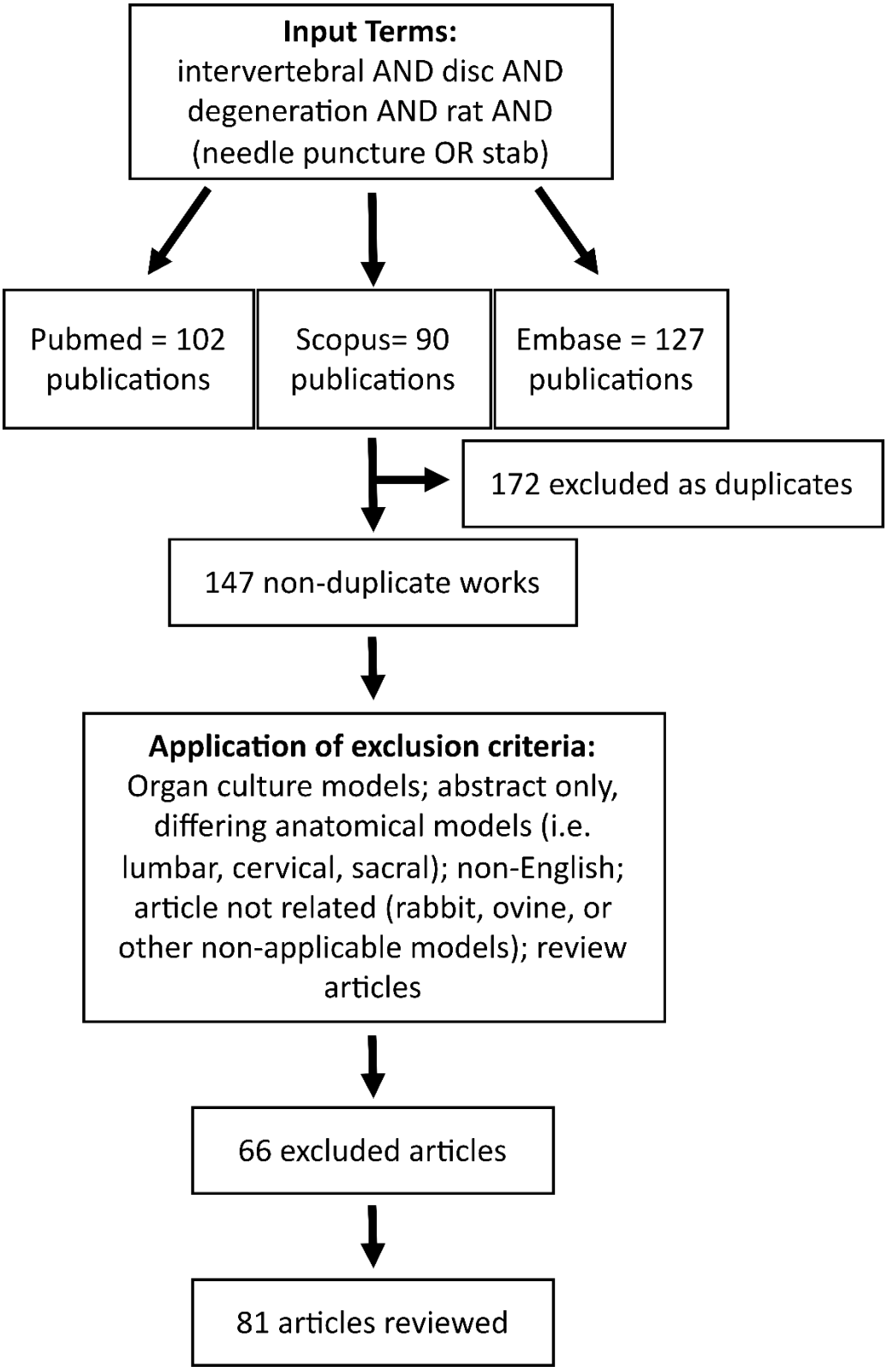

FIGURE 1: Preferred Reporting Items for Systematic Reviews and Meta-Analysis (PRISMA) diagram indicating the literature search terms, screening process, and exclusion criteria. One hundred and forty-six nonduplicate manuscripts were identified across PubMed, Scopus, and Embase on March 7, 2022. Following screening and the application of exclusion criteria, 80 articles were included in this review.

3 SUMMARY OF DATA FROM PEER REVIEWED MANUSCRIPTS

As shown in Figure **2A**, almost 90% of all papers reviewed used Wistar or Sprague Dawley rats for their studies (57/80 = 71.3% Sprague Dawley, 14/80 = 17.5% Wistar). Only four studies utilized Lewis rats (5.0%), while one study did not specify the rat strain. Four studies used nude rats (5.0%), which may be preferable or necessary for studies exploring delivery of agents associated with an increased risk of immune responses such as exogenous cell types. There appears to be significant consensus in terms of the age of the rats at the time of the study, with 12-week animals being used in 45 of 80 (56.3%) of all studies (Figure **2B**). Adulthood begins at ~8 weeks of postnatal life and 12-week-old rats are widely considered to be skeletally mature animals, while still retaining much of the juvenile phenotype.[22-25] This makes them good candidates for studies looking at disease progression versus aging, trauma, or other factors. There was also a considerably higher use of male rats (52/80 = 65.0%) than female rats (12/80 = 12.0%) (Figure **2C**). This may be due to the size difference between males and females, which may make both handling as well as intradiscal delivery procedurally easier. However, this bias could have negative implications as recent studies have found that sex differences exist both in disc degeneration as well as in the healing response following injury.[26] Although it is important to note that 16 studies (20%) did not specify the sex of the rats and these studies may account for additional single sex studies or mixed studies or both. Of the papers reviewed, 33 of 80 (41.3%) provided a local intradiscal treatment, 18 of 80 (22.5%) used systemic treatments and 24 of 80 (30.0%) involved developing a degeneration model and thus provided no treatment (Figure **2D**).

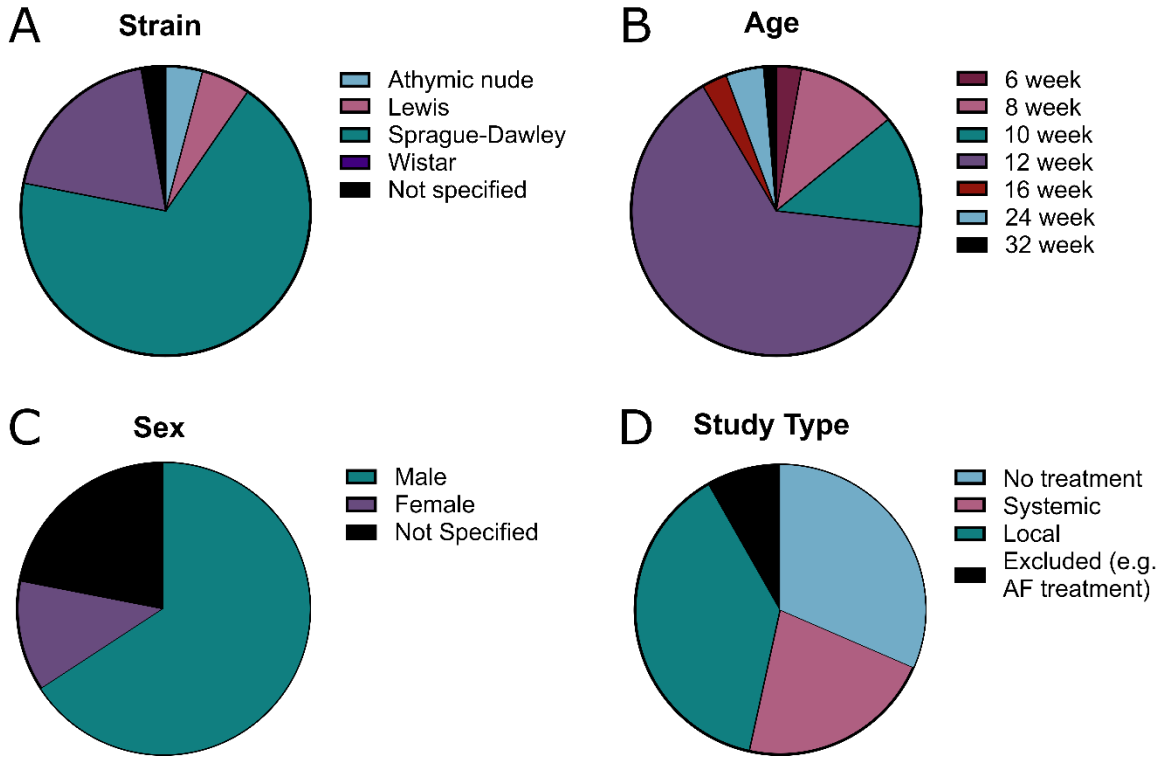

FIGURE 2: Summary of rat cohort, and the overall study design across the 80 articles reviewed. (A) The frequency of different rat strains used to create degeneration rat tail models (Sprague Dawley = 71.3%, Wister = 17.5%, Lewis = 5.0%, Athymic nude = 5.0% and 1.2% of studies did not specify rat strain). (B) Five studies (6.2%) used periadolescent rats at 6 weeks, while 26 studies (32.5%) used young adult rats at 8 and 10 weeks. However, most studies used rats older than 12 weeks, the timepoint at which skeletally maturity has occurred (12 weeks = 56.3%, 16 weeks = 1.3%, and 32 weeks = 2.5%). (C) Sixty-five percent of studies used male rats, while only 12.0% of studies used female rats. However, 20.0% of the studies did not specify the sex of the animals used. (D) 41.3% of studies investigated a treatment delivered locally within the degenerated disc, 22.5% focused on systemic delivery such as incorporation of drugs into food, or intraperitoneal injections, while 30.0% solely developed a degeneration model with no treatment delivery.

Disc geometry and scale is an important parameter to consider in animal models, particularly when relating preclinical results back to the human IVD. Furthermore, it may be important within the rat tail model design itself, for example, when comparing between a treatment and a control disc at different caudal levels. Figure **3A** highlights the number of discs used per animal and the frequency of each caudal level across the reviewed studies. Over 90% of the papers used three discs or fewer in their study, with 30 of 80 (37.5%) using one disc, 27 of 80 (33.8%) using two discs, and 17 of 80 (21.3%) using three discs per tail. Less than 8% used more than three discs, with six discs per animal being the greatest number reported. The caudal level reported in the literature ranged from C3–C4 to C9–C10. Despite seven studies not reporting the exact caudal levels used, there is a clear inclination toward discs between C5–C6 and C8–C9, with C7–C8 being the most frequently used disc (42 studies). We have carried out a geometrical analysis of rat tails (8-week-old Wistar rats [N = 6]) through histological slices in the transverse and sagittal plane. Figure **3B** shows the full disc diameter and the NP diameter

determined from the transverse plane. Moving distally along the rat tail there is a trend of decreasing disc size, with the diameter of C3–C4 more than 1 mm larger than the diameter of C9–C10. Although this may appear quite a small difference, when relating diameter to volume, this results in a 40%–60% decrease in disc volume (depending on disc height). A statistically significant difference between adjacent caudal levels was only found for the disc diameter between C4–C5 and C5–C6 ($p = 0.0048$). This is particularly interesting as it correlates well with the fact that most studies use discs within the C5–C6 to C8–C9 range, where our data suggests no significant difference in geometry among these discs. Figure **3C** shows a representative image of hematoxylin/eosin and picrosirius red/alcian blue staining of the most proximal and distal discs included in this review. Figure **3D** suggests very small differences in disc height between C3–C4 and C9–C10, with no statistical significance observed. However, from our experience larger decreases in disc height become rapidly apparent beyond disc C9–C10, with C10–C11 showing a significant difference in disc height compared to more proximal levels (data not shown as these discs were out of the caudal range reported in the literature and thus not pertinent to this review). Comparing this geometrical analysis to caudal discs from other species, we previously found little difference in bovine caudal disc diameter in the most proximal discs (C1–C2 to C5–C6), with differences only becoming significant at C6–C7. This is slightly more distal in the bovine tail than what was detected in the rat. However, unlike the rat analysis, significant differences in the central disc height of bovine caudal discs were found throughout the range C1–C2 through to C7–C8.[27]

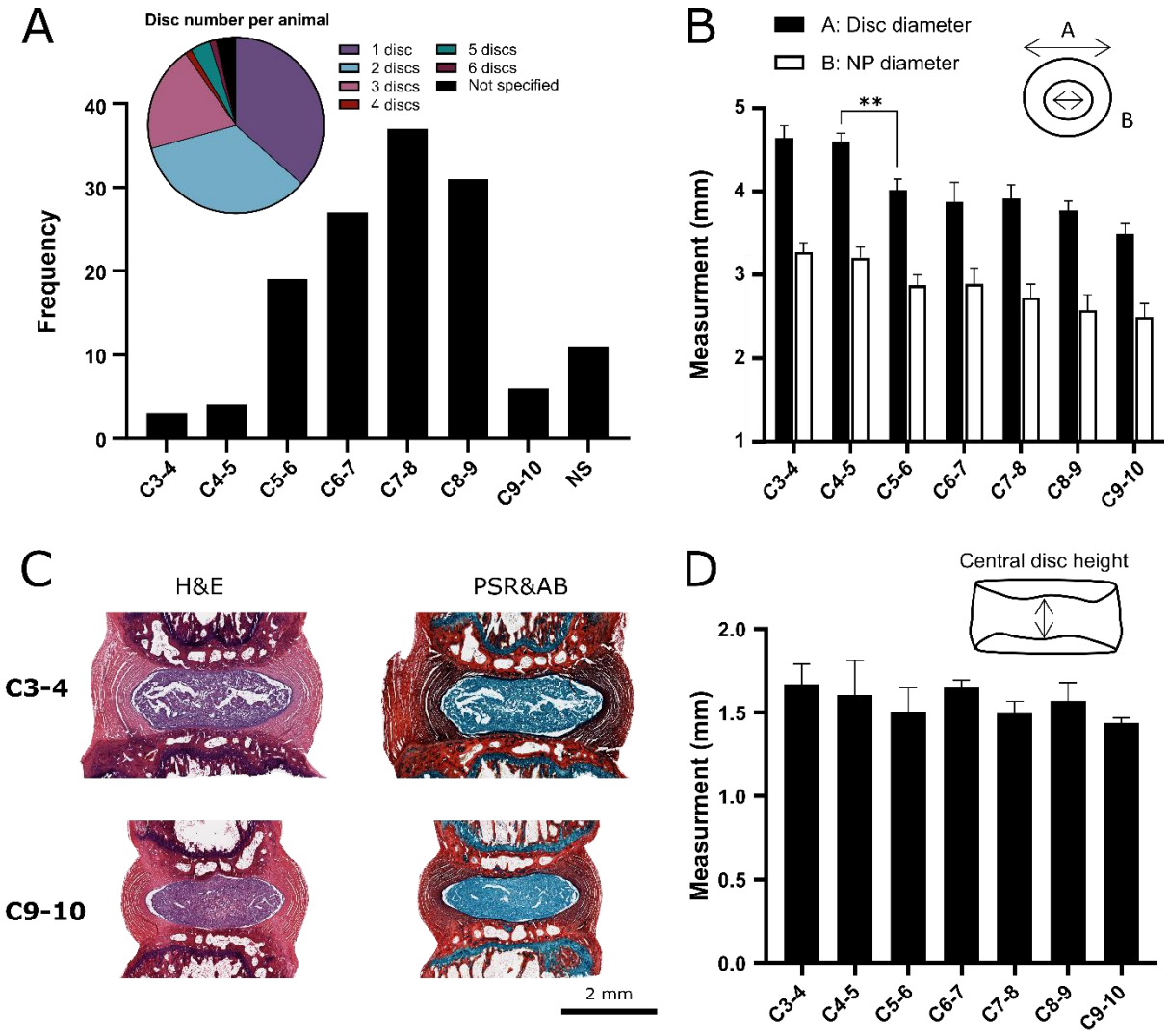

FIGURE 3: Anatomical and geometrical considerations. (A) The pie chart highlights the number of discs used per animal in each study, with most studies using 1 (37.5%), 2 (33.8%), or 3 (21.3%) discs. The bar graph shows the frequency and range of caudal levels used across these studies, with C7–C8 being the most frequent level and seven studies not specifying (NS) which discs were used. (B) Experimentally measured external disc diameter and internal nucleus pulposus (NP) diameter for 8-week-old Wister rats ($N = 6$). Statistics are only shown in the case of a statistical difference between adjacent levels with $p = 0.0048$. (C) Sagittal histology sections showing hematoxylin and eosin (H&E) and picrosirius red (PSR) combined with alcian blue (AB) for the most proximal and distal caudal discs investigated. (D) Experimentally measured central disc height, with no statistical significance found between adjacent levels within this range.

4 INDUCTION OF DEGENERATION

4.1 Commonly reported anesthetics and considerations

Minimizing anesthetic-related side effects is important both for animal welfare as well as reducing potential experimental interference or confounding factors.[28] Whether an inhalable or injectable anesthetic is used may be dictated by the experimental setup. In the case that injection is the preferred method, it is often recommended that either subcutaneous or intraperitoneal routes be used, as intramuscular injections may result in tissue irritation and may adversely

affect animal well-being. As shown in Figure **4A**, the three most reported anesthetic agents were pentobarbital (21/80 = 26.3%), isoflurane (17/80 = 21.3%), and ketamine–xylazine (14/80 = 17.5%). However, studies have demonstrated that ketamine–xylazine could induce abnormally slow heart rates and low arterial blood pressure when compared to pentobarbital, and lower heart rate and respiratory rate when compared to isoflurane.[28, 29] It has further been suggested that isoflurane had a nearly fivefold faster anesthetic induction time, a 2.5-fold faster recovery time, and a deeper anesthetic state than ketamine–xylazine as evidenced by fewer incidences of toe pinch responses while anesthetised.[29] An additional advantage of inhalable anesthetics over injectables is the ability to rapidly modify anesthetic exposure during the procedure.

4.2 Puncture induced degeneration model

As shown in Figure **4B**, three surgical approaches were reported: open surgery (22/80 = 27.5%), digital palpation of the IVD (36/80 = 45.0%), or fluoroscopically guided punctures (42/80 = 52.5%). However, it is important to note that studies often use a combination of these approaches. Fifteen studies used digital palpation and then confirmed the puncture using fluoroscopy while three studies carried out an open surgery under fluoroscopy. For illustrative purposes, Figure **4C**, demonstrates the fluoroscopically guided approach with microcomputed tomography (μCT) used to confirm the puncture of two caudal discs with a 25G and 27G needle. When using fluoroscopy, disc levels can be identified by imaging and counting down from the sacrum (with C1 being the first "free" vertebra following the four sacral vertebrae). If digital palpation is the preferred approach, disc levels can be identified by locating the processes along the vertebrae, with the last set of palpable processes reportedly found on the fifth caudal vertebra (i.e., level C5).[30] When conducting a pilot study to investigate puncture and treatment approaches, we compared open surgery with the disc exposed to percutaneous needle puncture through digital palpation to evaluate whether these two methods exhibited any differences. All procedures for this study were approved by the animal research ethics committee of Trinity College Dublin and the Health Products Regulatory Authority in Ireland (Approval-AE19136/P149). Briefly, 12-week-old Wistar rats ($n = 4$; 2 male and 2 female) were anesthetized with 2%–4% isoflurane with 1%–2% O_2. Meloxicam (1.5 mg/kg) was administered subcutaneously 1–2 h preoperatively. For the open surgery group, three caudal discs (C4–C5 through to C6–C7), in one male and one female rat, were exposed with a ~3 cm incision on the posterior caudal plane using a size 21 blade. Discs C4–C5 and C6–C7 were then punctured using a 21G needle, leaving disc C5–C6 intact. The puncture process involved inserting the needle intradiscally, rotating it 180 degrees, and holding it for 5 s before removing the needle. The skin was then sutured using 4-0 nylon sutures, animals were given a subcutaneous injection of buprenorphine (0.05 mg/kg), returned to their housing and allowed to recover. For the percutaneous punctures, discs C4–C5 through to C6–C7, for one male and one female rat, were identified via digital palpation and punctured through the skin using a 21G needle in the same manner as the open surgery, but following a percutaneous approach (i.e., without making an incision in the tail). Rats were likewise given a subcutaneous injection of buprenorphine prior to recovery. All rats were given daily injections of meloxicam (1.5 mg/kg) for 3 days following surgery.

Discs were imaged using μCT (Scanco VivaCT 80, 45 kVp, 177 μA, 8 W, and 78 μm voxel size) after 2 weeks to observe disc height (Figure **4D**). As shown in Figure **4E**, our data suggests that percutaneous punctures led to the same degree of IVD collapse and degeneration over the 2-week period. However, there was observably less inflammation near the puncture site in the percutaneous group than in the group with the open incision, likely leading to a lower degree of discomfort for the animals. Alternatively, we found that when delivering a treatment

into the disc, open surgery allowed for clear visualization of the disc and provided unobstructed confirmation of efficient intradiscal delivery, as well as retention of the therapy within the disc. Animal welfare should always be considered in the design of animal models. Thus, if two procedures are required (e.g., a needle puncture procedure for the induction of degeneration followed later by a second procedure to deliver a local treatment intradiscally), percutaneous puncture guided by digital palpation was found to be sufficient for the induction of degeneration. Then for the follow-up procedure, open surgery can be used to ensure proper treatment delivery, as mentioned previously. This approach eliminates the need for two open incisions in close temporal proximity of one another. This could be considered a valid refinement in animal welfare by diminishing pain and discomfort for the animal and reducing the potential for surgical complications such as infection.

4.3 Selection of needle gauge size

For the induction of degeneration, previous published work suggests that needle gauges smaller than 23G did not produce consistent and significant degrees of degeneration in rat which was confirmed through magnetic resonance imaging (MRI).[31] Work conducted in a mouse model previously suggested that needle diameters >40% of disc height were necessary to alter disc function in the lumbar spine.[32] This hypothesis was further investigated in rat models, where similar trends in the loss of mechanical function, loss of signal intensity and MRI indices, and loss in histological structures were observed following punctures with needle gauges ranging from 18G to 27G.[33-36] A study by Keorochana et al. further suggested that needle size affects not only the degree of degeneration but also the rate of degeneration.[36] The authors investigated the effects of 18G, 20G, and 21G needles each in C6–C7 and C7–C8 discs (all >40% of the disc height). The 18G needle puncture promoted significant differences in disc height index at all time points, and greater differences became apparent over time. MRI revealed significant degrees of degeneration at early time points (i.e., 2 weeks) only in the 18G needle puncture group. 20G needles promoted degeneration that became apparent at intermediate time points (4, 6, and 8 weeks), while 22G needle puncture only demonstrated effects at the 8-week time point. Histological evaluations corroborated those findings.

As highlighted in Figure **4F**, we found that a significant majority of studies in our review adhered to these findings, with 28 studies inducing degeneration using a 21G needle, 20 studies with a 20G needle and 17 studies using an 18G needle. One point for discussion is the degree of degeneration desired. Whether mild degeneration or complete destruction of the disc is desired is entirely dependent on the experimental design and the scientific question or objective of the study. The inset graph highlights the outer diameter of each needle gauge, as well as relating it to disc height (assuming a disc height of 1.5 mm) to better inform design choices. For example, assuming an average caudal disc height of 1.5 mm, puncture with a large needle gauge such as an 18G (average outer diameter of ~1.25 mm, ~80% disc height) may lead to complete destruction of the IVD rather than mild degeneration and may thus interfere with studies seeking to provide long-term disc restabilization or regenerative tissue engineering models. Alternatively, if severe defect formation is needed for the proposed model, puncture with a 27G needle (average outer needle diameter of ~0.4 mm, ~25% disc height) would not likely be sufficient and a larger needle may be necessary.

5 TREATMENT OF DEGENERATION

5.1 Timepoint and type of treatment

Our review found that 32 studies provided treatment immediately following puncture (Figure **4G**). Of those, 18 studies provided a local IVD treatment, while 7 studies focused on systemic delivery such as incorporation of drugs into food, or intraperitoneal injections. Twenty-four studies provided no treatment but focused on the study of different parameters associated with progression of IVD degeneration. It is worth discussing that whether treatment is delivered following the onset of acute disc degeneration or immediately following puncture may be dependent on the research question being investigating. For example, research on how a therapeutic slows down degeneration and treatments for restoring mechanical function in a degenerative disc are likely to require different experimental setups, and thus the outcomes may be impacted by improper design. Thus, careful consideration of treatment delivery as a factor of research outcomes of interest is of importance.

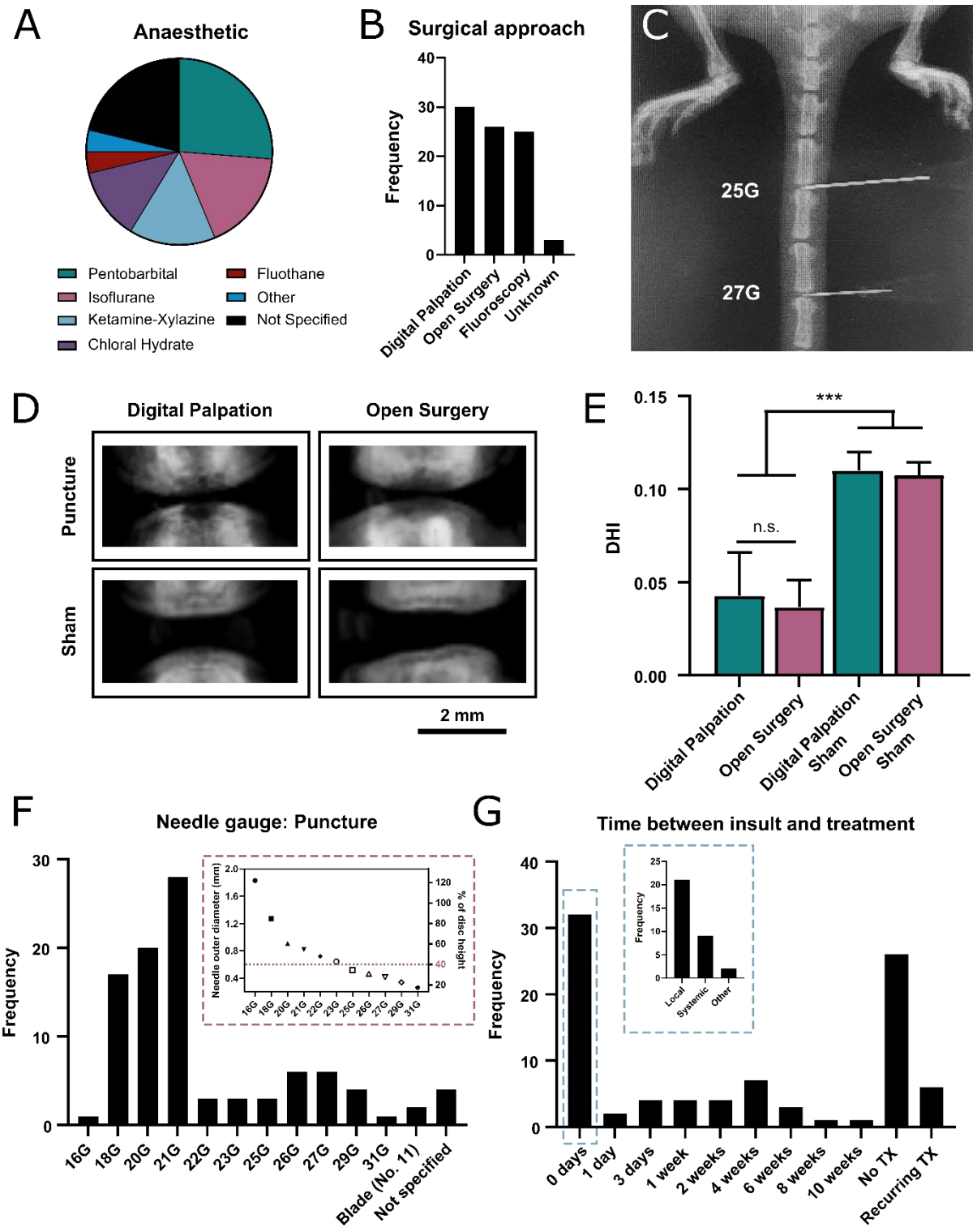

FIGURE 4: Surgical approaches to establishing a degeneration rat tail model. (A) The majority of studies used pentobarbital (21/80 = 26.3%), isoflurane (17/80 = 21.3%), or ketamine–xylazine (14/80 = 17.5%). Less than 20% of studies used an alternative anesthetic; chloral hydrate, fluothane or other (medetomidine, midazolam, butorphanol, pelltobarbitalum natricum, or atipamezole). However, 13 studies (16.1%) did not report the anesthetic used. (B) The frequency of either digital palpation, open surgery, or fluoroscopically guided punctures used across the reviewed studies. (C) A microcomputed tomography (μCT) image demonstrating the fluoroscopically guided approach used to confirm the needle position. (D) μCT images to observe the reduction in disc height 2 weeks following subcutaneously puncture through digital palpation and open surgery. (E) Quantitative analysis using

disc height index (DHI) to compare the effect of percutaneous puncture and open surgery ($p < 0.003$). (F) The frequency of needle gauges used to puncture the disc across the reviewed studies. The inset graph relates the outer needle diameter of each needle gauge to disc height, assuming an average disc height of 1.5 mm (G) The time between puncture insult and treatment (TX) across the reviewed studies.

5.2 Needle gauges and volumes delivered

Treatments are commonly administered through a 31G needle (Figure **5A**) as the outer diameter of the needle is <20% of a rat disc height and is unlikely to promote further degeneration.[31] However, a caveat to this needle diameter is that it may present complications in the delivery of biomaterials, as parameters such as viscosity/density and shear may impact the feasibility of material delivery and extrusion through this needle gauge. This may result in lower gauge (wider bore) needles being better candidates for biomaterial delivery. Focusing on the studies that provided a local treatment delivery into the intradiscal space, Figure **5B** shows that most studies reported an injection volume of 2 μl (20 studies). To better estimate NP volume, we obtained six caudal spines from freshly euthanised Wistar rats (male, 20 weeks old) and extracted the NP of six discs per rat (C4–C5 through to C9–C10) by cutting the discs along the transverse plane at the superior CEP, and then removed the gelatinous NP tissue using needle-point forceps. We weighed the extracted NP tissue and measured 3.1 ± 0.5 mg per disc. Assuming hydration ranges between 70% and 90%, this would roughly equate to volumes between 2 and 3 μl. It may thus follow that the reported injected volumes of 2–5 μl may be best suited for intradiscal treatment delivery without causing detrimental changes in intradiscal pressure.

5.3 Cellular versus acellular treatment

Again, focusing on the studies that provided a local treatment delivery into the intradiscal space, 28 studies used an acellular approach and 5 used a cell-based treatment. Although two studies compared both a cellular and an acellular approach. Figure **5C** highlights that among the cellular approaches, there does not appear to be a consensus on the cell number to be delivered as within our sample size of five reviewed papers, we observed values ranging from 2000 to 150 000 cells/disc (assuming a NP or injection volume of 2 μl; this range is equivalent to 1 million to 75 million cells/ml). It is typically reported that the native human NP cell densities is ~4 million cells/ml.[37] However, more recent work assessing cell density with respect to degeneration grade have reported the total NP cell density to be closer to ~2.5 million cells/ml (depending on specific grade of interest) and out of the total cell population only ~1.3 million cells/ml appear to be metabolically active.[38] In comparison, native NP cell densities for rat discs have been reported as high as 80 million cells/ml in adult Sprague Dawley rats.[39] This suggests that more deliberate consideration is needed in the design of cellular treatments. It is important to assess whether the aim is to fully replace the NP with a biomaterial which matches the native density of the tissue, or whether the therapeutic aims to aid and stimulate inherent regeneration of the native NP. In the case of the latter, it may be important to consider the total cell number already resident in the rat NP and how many more cells can be implanted without further exacerbating the degenerative niche and in turn affecting the viability and regenerative potential of the treatment.[40] Furthermore, given the significant differences in rat and human NP cell density, it may be important to take this into consideration at an earlier stage of design and testing, to assist not only in the progression to large animal models but to help realize more successful clinical translation.

6 PRIMARY OUTCOME MEASURES

According to Figure **5D** a similar number of studies evaluated the outcome measures at 1–2 weeks (36 studies), 3–4 weeks (36 studies), and >8 weeks (41 studies). It is worth noting that most studies used multiple timepoints to allow for temporal comparisons. These timepoints are likely recurrent as they may be representative of the progression of pathology from acute to intermediate and chronic stages of IVD degeneration.[41]

Figure **5E** shows the frequency of different outcome measures used throughout the reviewed literature. For longitudinal or temporal studies, where in vivo data was to be collected throughout the study, MRI (53 studies) and μCT (37 studies) are the predominant outcome measures reported in the literature. Although these measures were also popular in terminal timepoint studies. However, in postmortem, histological analysis (75 studies) was the most popular evaluation metric. Immunohistochemistry (39 studies) was another popular approach, as it provides a level of biologically relevant detail that is not necessarily attainable with standard histological techniques. Furthermore, recent work by Lai et al. proposed a standardized method for histopathology scoring, which may further support the path toward consistent experimental development.[42] Within the subset of papers that employed immunohistochemistry as an outcome measure, Figure **5F**, the most popularly reported targets were associated with either extracellular matrix deposition, specifically collagen II (18 studies), aggrecan (12 studies), MMP3 (7 studies), and MMP13 (5 studies), or markers associated with an inflammatory response, specifically IL-1β (7 studies) and TNF-α (5 studies). While tissue biomechanics are an important factor to consider in tissue regeneration approaches, only four reviewed works reported mechanical testing data. This is likely due to these experiments most often being utilized in organ culture models due to reduced confounding factors and a subsequent ability to obtain clearer outputs. Radiographic, MRI, and histological analyses all captured the progression of degeneration as evidenced by differences in disc height and structure compared to control discs, as early as 2 weeks.

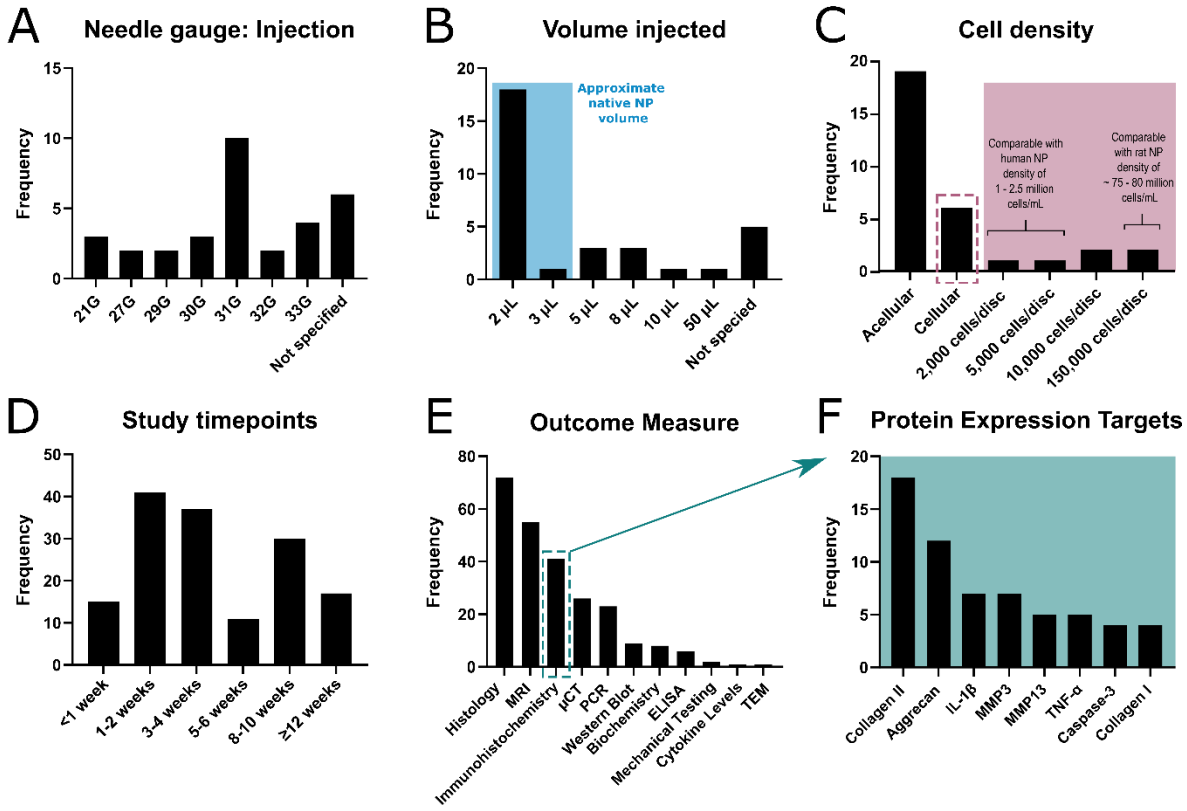

FIGURE 5: Treatment parameters and outcome measures used in the reviewed rat tail models. (A) Treatments are commonly administered through a 31G needle (10 papers). However, six papers failed to report on the needle gauge used. (B) Most studies reported an injection volume of 2 µl (20 studies), which is within the approximated rat NP volume estimated from NP tissue weights and accounting for hydration, blue overlay. (C) The majority of reviewed studies used an acellular approach (28 studies). Within the studies that used a cell-based treatment (five studies) the cell densities varied extensively. Assuming a 2 µl NP volume, these cell densities have been compared to the native cell densities of the human and rat NP. (D) The literature reported a range of timepoints, with 1–2 weeks and 3–4 weeks the most popular for early timepoints and >8 weeks typical for later timepoints. (E) The frequency of different outcome measures used throughout the reviewed literature. (F) The most common protein expression targets determined through immunohistochemistry.

7 ASSOCIATED LIMITATIONS WITH RAT TAIL MODELS

The objective of this review is to provide a summary of the parameters most employed to establish a rat caudal degeneration model. One significant advantage of the caudal model is the ease of access and high throughput nature. It can help in the interpretation of data as results are less likely to be confounded by the loadings observed in the lumbar spine, particularly at an early stage of therapeutic development, before transitioning to a larger, more anatomically relevant animal model. However, limitations do exist. For example, lumbar models offer more biological complexity, and more physiological relevance in terms of biomechanical parameters. Thus, lumbar models may be more useful to researchers seeking to study neoinnervation and vascularization or subsequent immune or inflammatory responses and their associations with the pain phenotype. Caudal models may present challenges as exposure to neural and vascular microenvironments differs from other anatomical regions such as the lumbar spine. As mentioned previously disc scale is an important parameter to consider in rat

models, particularly when relating preclinical results back to the larger avascular human IVD with its unique microenvironment,[40] which is often speculated to be linked to the high failure of perspective studies.[43-45] Correlation of metrics from rat models toward human applications is difficult due to a number of characteristic differences between the two. For example, a key difference can be observed in terms of cell populations. Humans have been observed to undergo a significant transition of notochordal cells toward nucleopulpocytes, resulting in a near depletion of notochordal cells by age 10.[2, 14, 46] However, these changes are less abrupt in rat IVDs, with populations of notochordal cells still being observed into skeletal maturity and adulthood.[14, 47] Another key difference involves vascularization at early stages of development. In humans, significant decreases in vascularization have been observed in childhood as early as age 4, with the discs becoming further avascular with aging.[39, 48] By contrast, while a decrease in vascular body presence was likewise observed with aging in rats, this was not observed until late adulthood (22 months in rats).[49] Taken together, these factors suggest that more in depth knowledge is needed on the microenvironmental niche created within these rat tail models, particularly in the case of nutrient demands and availability to ensure that cell-based therapies are being tested under robust and clinically relevant conditions. Finally, another limitation involves the study of the pain phenotype. While some studies (9/80 = ~11%) discussed a focus on the quantification of pain-related markers such as differential cytokine levels, only one study among all reviewed papers conducted behavioral analysis for pain-related metrics. Behavioral analysis is often reported in lumbar models of radiculopathy but are less prominent in caudal models due to the reduced nerve presence by comparison. Nevertheless, due to the importance of gaining a better understanding of the pain phenotype, this may be a significant limitation of using caudal models.

8 CONCLUSION

Rat caudal models of disc degeneration have demonstrated significant utility in the study of disease progression and its impact on tissue structure, composition, and mechanical performance. While different models may yield different experimental outcomes, a considerable number of studies utilize a physical insult by means of needle puncture to induce degeneration. Although previous work, such as that by Elliott et al.,[32] have provided meaningful information toward consistent and reproducible induction of degeneration in rodent models, the literature still maintains significant variability in these approaches. Caudal models offer benefits in terms of surgical procedures since a less invasive approach is needed for a caudal disc puncture compared to other anatomical regions. The use of caudal models further enables the researcher to create percutaneous tissue insults to initiate disc degeneration without the need for an open surgery, which in turn, may improve overall animal well-being and decrease the risk for surgical complications.

Figure **6** visually summarizes the main findings of this review. In the case that multiple surgical procedures are required, as is the case for experiments where the induction of degeneration and its treatment are temporally distinct, induction of degeneration using a percutaneous puncture is recommended as it may lead to improved animal welfare overall. For the intradiscal delivery of a treatment group, an open surgery may be the best approach as it allows for full visualization and confirmation of effective delivery into the disc. The use of a 31G needle for treatment delivery was the most popular choice, although needle gauges as large as 27G have been used without observable or significant changes to the disc structure or contribution to disease progression. These ranges may be beneficial for drug-based treatments, but more consideration

may be necessary when delivering viscous biomaterials as their extrusion may become hindered at higher gauges.

For the induction of degeneration via needle puncture, different approaches may be selected. Needle gauges of 25G–23G (~0.5–0.6 mm outer diameter and ~35%–45% of the disc height, respectively) may be best suited for the induction of acute degeneration in accordance with size ratios previously reported in the literature, while gauges of 21G–18G (~0.8–1.3 mm outer diameter and ~55%–85% of the disc height, respectively) may be better suited for a more aggressive defect. Likewise, time between insult and treatment may depend on the specific research question as the degree of degeneration within the disc prior to delivery of a treatment will have significant impact in the experimental outcomes. Furthermore, delivery of intradiscal volumes between 2 and 5 µl is advised, as this range falls within the observed and reported dimensions of NP tissue (with a margin for error) and would allow for effective delivery with minimal effects on intradiscal pressure. For the length of treatment application following induction of degeneration, timepoints of 1–2, 3–4, and 8–10 weeks were most often selected as measures of early, intermediate, and late-stage disc degeneration.

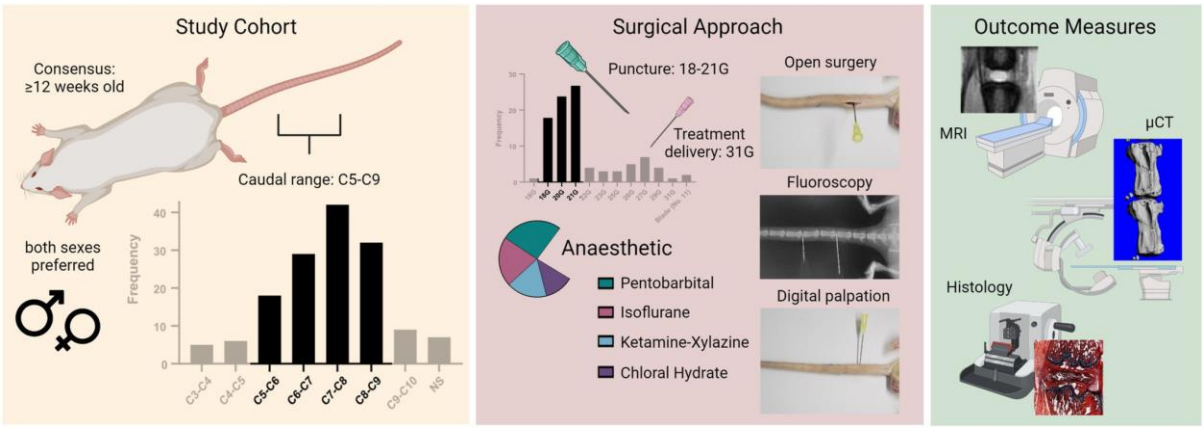

FIGURE 6: A visual summary of the main findings compiled from the reviewed rat tail models. There is a general consensus to use rats at least 12 weeks old to ensure skeletal maturity, and both sexes are preferred. Most studies operate within the C5–C9 range. 18–21G needles are preferred for inducing degeneration, while a 31G needle is preferred for intradiscal treatment delivery. Pentobarbital and isoflurane are the favored anesthetics, followed by ketamine–xylazine and chloral hydrate. The surgical approach may be based on the specific experimental design and can include open surgery, fluoroscopy, and digital palpation. The most reported outcome measures were magnetic resonance imaging (MRI), microcomputed tomography (µCT) and histology. Created with BioRender.com.

AUTHOR CONTRIBUTIONS

All authors contributed to the conception and design of the work. Marcos N. Barcellona, Emily E. McDonnell, and Shani Samuel performed the acquisition, analysis, and interpretation of literature data. Marcos N. Barcellona and Emily E. McDonnell preformed the pilot rat study, acquisition, analysis, presentation, and interpretation of results, drafting of the article, revising it critically and final approval. Conor T. Buckley, as the overall project funding holder, takes responsibility for the integrity of the work from inception to finalized article, provided

substantial contribution to data interpretation and presentation, drafting of the article, revising it critically, and final approval.

ACKNOWLEDGMENTS

The authors would also like to thank Rustam Rakhmatullin, Christian Kerskens, Daniel Ruiz Perez and the Comparative Medicine Unit (CMU) staff at TCD for their continued technical assistance and support. This work was supported by a Science Foundation Ireland Career Development Award (15/CDA/3476). Open access funding provided by IReL. WOA Institution: The University of Dublin Trinity College Consortia Name: IReL gold OA 2022

CONFLICT OF INTEREST

The authors declare no conflicts of interest.

REFERENCES

1 Setton LA, Chen J. Mechanobiology of the intervertebral disc and relevance to disc degeneration. J Bone Joint Surg Am. 2006; 88(2): 52- 57.

2 Trout JJ, Buckwalter JA, Moore KC, Landas SK. Ultrastructure of the human intervertebral disc. I. Changes in notochordal cells with age. Tissue Cell. 1982; 14(2): 359- 369.

3 Shankar H, Scarlett JA, Abram SE. Anatomy and pathophysiology of intervertebral disc disease. Tech Reg Anesth Pain Manag. 2009; 13(2): 67- 75. doi:10.1053/J.TRAP.2009.05.001

4 Adams P, Eyre DR, Muir H. Biochemical aspects of development and ageing of human lumbar intervertebral discs. Rheumatology. 1977; 16(1): 22- 29.

5 Roberts S, Menage J, Urban JPG. Biochemical and structural properties of the cartilage end-plate and its relation to the intervertebral disc. Spine (Phila pa 1976). 1989; 14(2): 166- 174.

6 Moore RJ. The vertebral endplate: disc degeneration, disc regeneration. Eur Spine J. 2006; 15: 333- 337. doi:10.1007/s00586-006-0170-4

7 Lotz JC, Fields AJ, Liebenberg E. The role of the vertebral end plate in low back pain. Glob Spine J. 2013; 3(3): 153- 164.

8 Iatridis JC, Setton LA, Weidenbaum M, Mow VC. Alterations in the mechanical behavior of the human lumbar nucleus pulposus with degeneration and aging. J Orthop Res. 1997; 15(2): 318- 322. doi:10.1002/JOR.1100150224

9 Urban JPG, Roberts S. Degeneration of the intervertebral disc. Arthritis Res Ther. 2003; 5(3): 120- 130.

10 Roughley PJ. Biology of intervertebral disc aging and degeneration: involvement of the extracellular matrix. Spine (Phila pa 1976). 2004; 29(23): 2691- 2699. doi:10.1097/01.brs.0000146101.53784.b1

11 Chen J, Jing L, Gilchrist CL, Richardson WJ, Fitch RD, Setton LA. Expression of laminin isoforms, receptors, and binding proteins unique to nucleus pulposus cells of immature intervertebral disc. Connect Tissue Res. 2009; 50(5): 294- 306.

12 Iatridis JC, Weidenbaum M, Setton LA, Mow VC. Is the nucleus Pulposus a solid or a fluid? Mechanical behaviors of the nucleus pulposus of the human intervertebral disc. Spine (Phila pa 1976). 1996; 21(10): 1174- 1184.

13 Ashinsky B, Smith HE, Mauck RL, Gullbrand SE. Intervertebral disc degeneration and regeneration: a motion segment perspective. Eur Cell Mater. 2021; 41: 370- 380. doi:10.22203/eCM.v041a24

14 Fusellier M, Clouet J, Gauthier O, Tryfonidou MA, Le Visage C, Guicheux J. Degenerative lumbar disc disease: in vivo data support the rationale for the selection of appropriate animal models. Eur Cells Mater. 2020; 39: 18- 47. doi:10.22203/eCM.v039a02

15 Daly C, Ghosh P, Jenkin G, Oehme D, Goldschlager T. A review of animal models of intervertebral disc degeneration: pathophysiology, regeneration, and translation to the clinic. Biomed Res Int. 2016; 2016:5952165.

16 Hunter C, Matyas J, Duncan NA. The notochordal cell in the nucleus pulposus: a review in the context of tissue engineering. Tissue Eng. 2003; 9(4): 667- 677.

17 Choi H, Tessier S, Silagi ES, et al. A novel mouse model of intervertebral disc degeneration shows altered cell fate and matrix homeostasis. Matrix Biol. 2018; 70: 102- 122. doi:10.1016/j.matbio.2018.03.019.A

18 Choi KS, Lee C, Harfe BD. Sonic hedgehog in the notochord is sufficient for patterning of the intervertebral discs. Mech Dev. 2012; 129(9-12): 255- 262. doi:10.1016/J.MOD.2012.07.003

19 Gullbrand SE, Ashinsky BG, Bonnevie ED, et al. Long-term mechanical function and integration of an implanted tissue engineered intervertebral disc. Sci Transl Med. 2018; 10(468):eaau0670. doi:10.1126/SCITRANSLMED.AAU0670

20 Gullbrand SE, Schaer TP, Agarwal P, et al. Translation of an injectable triple-interpenetrating-network hydrogel for intervertebral disc regeneration in a goat model. Acta Biomater. 2017; 60: 201- 209. doi:10.1016/j.actbio.2017.07.025

21 Moher D, Liberati A, Tetzlaff J, Altman DG. Preferred Reporting Items for Systematic Reviews and Meta-Analyses: the PRISMA statement. BMJ. 2009; 339:b2535. doi:10.1136/bmj.b2535

22 Kember N. Aspects of the maturation process in growth cartilage in the rat tibia. Clin Orthop. 1973; 95: 288- 294.

23 Hunziker EB, Schenk RK. Physiological mechanisms adopted by chondrocytes in regulating longitudinal bone growth in rats. J Physiol. 1989; 414: 55- 71.

24 Roach HI, Mehta G, Oreffo ROC, Clarke NMP, Cooper C. Temporal analysis of rat growth plates: cessation of growth with age despite presence of a physis. J Histochem Cytochem. 2003; 51: 373- 383.

25 Hunter CJ, Matyas J, Duncan NA. The three-dimensional architecture of the notochordal nucleus pulposus: novel observations on cell structures in the canine intervertebral disc. J Anat. 2003; 202: 279- 291.

26 Mosley GE, Hoy RC, Nasser P, et al. Sex differences in rat intervertebral disc structure and function following annular puncture injury. Spine (Phila pa 1976). 2019; 44(18): 1257- 1269. doi:10.1097/BRS.0000000000003055

27 McDonnell EE, Buckley CT. Investigating the physiological relevance of ex vivo disc organ culture nutrient microenvironments using in silico modeling and experimental validation. JOR Spine. 2021; 4(2):e1141. doi:10.1002/jsp2.1141

28 Shekarforoush S, Fatahi Z, Safari F. The effects of pentobarbital, ketamine–pentobarbital and ketamine–xylazine anesthesia in a rat myocardial ischemic reperfusion injury model. Lab Anim. 2016; 50(3): 179- 184. doi:10.1177/0023677215597136

29 Jiron JM, Calle JLM, Castillo EJ, et al. Comparison of isoflurane, ketamine-dexmedetomidine, and ketamine-xylazine for general anesthesia during oral procedures in rice rats (Oryzomys palustris). J Am Assoc Lab Anim Sci. 2019; 58(1): 40- 49. doi:10.30802/AALAS-JAALAS-18-000032

30 Than KD, Rahman SU, Wang L, et al. Intradiscal injection of simvastatin results in radiologic, histologic, and genetic evidence of disc regeneration in a rat model of degenerative disc disease. Spine J. 2014; 14(6): 1017- 1028. doi:10.1016/j.spinee.2013.11.034.Intradiscal

31 Zhang H, La Marca F, Hollister SJ, Goldstein SA, Lin CY. Developing consistently reproducible intervertebral disc degeneration at rat caudal spine by using needle puncture: laboratory investigation. J Neurosurg Spine. 2009; 10(6): 522- 530. doi:10.3171/2009.2.SPINE08925

32 Martin JT, Gorth DJ, Beattie EE, Harfe BD, Smith LJ, Elliott DM. Needle puncture injury causes acute and long-term mechanical deficiency in a mouse model of intervertebral disc degeneration. J Orthop Res. 2013; 31(8): 1276- 1282. doi:10.1002/JOR.22355

33 Elliott DM, Yerramalli CS, Beckstein JC, Boxberger JI, Johannessen W, Vresilovic EJ. The effect of relative needle diameter in puncture and sham injection animal models of degeneration. Spine (Phila pa 1976). 2008; 33(6): 588- 596. doi:10.1097/BRS.0B013E318166E0A2

34 Hsieh AH, Hwang D, Ryan DA, Freeman AK, Kim H. Degenerative anular changes induced by puncture are associated with insufficiency of disc biomechanical function. Spine (Phila pa 1976). 2009; 34(10): 998- 1005. doi:10.1097/BRS.0B013E31819C09C4

35 Michalek AJ, Funabashi KL, Iatridis JC. Needle puncture injury of the rat intervertebral disc affects torsional and compressive biomechanics differently. Eur Spine J. 2010; 19: 2110-2116. doi:10.1007/s00586-010-1473-z

36 Keorochana G, Johnson JS, Taghavi CE, et al. The effect of needle size inducing degeneration in the rat caudal disc: evaluation using radiograph, magnetic resonance imaging, histology, and immunohistochemistry. Spine J. 2010; 10(11): 1014- 1023. doi:10.1016/J.SPINEE.2010.08.013

37 Maroudas A, Stockwell R, Nachemson A, Urban JPG. Factors involved in the nutrition of the human lumbar intervertebral disc: cellularity and diffusion of glucose in vitro. J Anat. 1975; 120(1): 113- 130.

38 Liebscher T, Haefeli M, Wuertz K, Nerlich AG, Boos N. Age-related variation in cell density of human lumbar intervertebral disc. Spine (Phila pa 1976). 2011; 36(2): 153- 159.

39 Miyazaki T, Kobayashi S, Takeno K, Meir A, Urban JPG, Baba H. A phenotypic comparison of proteoglycan production of intervertebral disc cells isolated from rats, rabbits, and bovine tails; which animal model is most suitable to study tissue engineering and biological repair of human disc disorders? Tissue Eng Part A. 2009; 15(12): 3835- 3846. doi:10.1089/ten.tea.2009.0250

40 McDonnell EE, Buckley CT. Consolidating and re-evaluating the human disc nutrient microenvironment. JOR Spine. 2022; 5(1):e1192. doi:10.1002/JSP2.1192

41 Leimer EM, Gayoso MG, Jing L, Tang SY, Gupta MC, Setton LA. Behavioral compensations and neuronal remodeling in a rodent model of chronic intervertebral disc degeneration. Sci Rep. 2019; 9(1):3759. doi:10.1038/s41598-019-39657-6

42 Lai A, Gansau J, Gullbrand SE, et al. Development of a standardized histopathology scoring system for intervertebral disc degeneration in rat models: an initiative of the ORS spine section. JOR Spine. 2021; 4(2):e1150. doi:10.1002/jsp2.1150

43 Sakai D, Andersson GBJ. Stem cell therapy for intervertebral disc regeneration: obstacles and solutions. Nat Rev Rheumatol. 2015; 11(4): 243- 256. doi:10.1038/nrrheum.2015.13

44 Farhang N, Silverman LI, Bowles RD. Improving cell therapy survival and anabolism in harsh musculoskeletal disease environments. Tissue Eng Part B Rev. 2020; 26(4): 348- 366. doi:10.1089/ten.teb.2019.0324

45 Smith LJ, Silverman LI, Sakai D, et al. Advancing cell therapies for intervertebral disc regeneration from the lab to the clinic: recommendations of the ORS spine section. JOR Spine. 2018; 1(4):e1036. doi:10.1002/jsp2.1036

46 Smith LJ, Nerurkar NL, Choi K-S, Harfe BD, Elliott DM. Degeneration and regeneration of the intervertebral disc: lessons from development. Dis Model Mech. 2011; 4(1): 31- 41.

47 Elliott DM, Sarver JJ. Young investigator award winner: validation of the mouse and rat disc as mechanical models of the human lumbar disc. Spine (Phila pa 1976). 2004; 29(7): 713-722. doi:10.1097/01.BRS.0000116982.19331.EA

48 Fournier DE, Kiser PK, Shoemaker JK, Battié MC, Séguin CA. Vascularization of the human intervertebral disc: a scoping review. JOR Spine. 2020; 3(4):e1123. doi:10.1002/jsp2.1123

49 Zhang YG, Sun ZM, Liu JT, Wang SJ, Ren FL, Guo X. Features of intervertebral disc degeneration in rat's aging process. J Zhejiang Univ Sci B. 2009; 10(7): 522- 527. doi:10.1631/jzus.B0820295

SUPPORTING INFORMATION

Table S1 List of reviewed manuscripts and relevant experimental details extracted from the literature

DOI	Author and Year	Title	Number of rats	Age (weeks); Sex (M/F)	Strain	Anesthetic	Number of discs punctured; disc level	Procedure approach	Time from induction of degeneration to treatment	Treatment details (if applicable)	Time from degeneration to euthanasia	Outcome measures
10.1016/j.jot.2021.04.003	Wu et al., 2021	Krüppel like factor 10 prevents intervertebral disc degeneration via TGF-β signaling pathway both in vitro and in vivo	24	12; M	Sprague-Dawley (SD)	Chloral hydrate	1; C7-C8	Digital palpation, percutaneous puncture with 21G needle to depth of 5 mm	Immediately after insult	Intradiscal; 10 µL, no needle gauge specified	Euthanasia 8 weeks after initial puncture	X-ray, MRI, histology, immunohistochemistry (IHC)
10.1002/ar.24519	Fattah & El-Din, 2021	Granulocyte-colony stimulating factor improves intervertebral disc degeneration in experimental adult male rats: A microscopic and radiological study	36	12; M	SD	Ketamine-Xylazine	2; C5-C6, C7-C8	Open surgery, puncture with 20G needle to depth of 5 mm	6 weeks after insult	Systemic (subcutaneous treatment delivery)	Euthanized 8 weeks after puncture	X-ray, histology, IHC, TEM
10.1155/2021/6672978	Dai et al., 2021	Salvianolic Acid B Protects Intervertebral Discs from Oxidative Stress-Induced Degeneration via Activation of the JAK2/STAT3 Signaling Pathway	60	No specified age or weight; M	SD	Fluothane in oxygen/nitrous oxide	1; C8-C9	Digital palpation, percutaneous disc puncture with 20G needle to depth of 5 mm	Treatment delivered following surgery	Systemic (oral gavage)	Euthanized 6 weeks after puncture	MRI, histology, biochemical analysis, ELISA, western blotting
10.1155/2021/6631562	Zhang et al., 2021	Quercetin Alleviates Intervertebral Disc Degeneration by Modulating p38 MAPK-Mediated Autophagy	36	8; M	SD	Pentobarbital	no details	Fluoroscopy guided percutaneous puncture with 27G needle to depth of 4 mm	Immediately after insult	Systemic (intragastric delivery)	Euthanized 8 weeks after puncture	MRI, histology, IHC, western blotting
10.1155/2021/5510124	Tian et al., 2021	Intervertebral Disc Degeneration Induced by Needle Puncture and Ovariectomy: A Rat Coccygeal Model	Stage 1: 36; Stage 2: 9	12; F	SD	Pentobarbital	3; C5-C6 to C7-C8	Open surgery, puncture with 21G needle to depth of 3 mm	Immediately after insult	Systemic (subcutaneous delivery)	Euthanized at 4, 8 and 12 weeks after puncture	Micro-MRI, histology
10.1155/2021/5556122	Dai et al., 2021	Sodium Tanshinone IIA Sulfonate Ameliorates Injury-Induced Oxidative Stress and Intervertebral Disc Degeneration in Rats by Inhibiting p38 MAPK Signaling Pathway	40	12; M	SD	Fluothane in oxygen/nitrous oxide	1; C8-C9	Digital palpation, percutaneous disc puncture with 20G needle to depth of 5 mm	Immediately after insult	Systemic (intraperitoneal delivery)	Euthanized 4 weeks after puncture	X-ray, MRI, histology, IHC, ELISA, western blotting
10.1002/jor.24757	Nakashima et al., 2020	Quantitative analysis of intervertebral disc degeneration using Q-space imaging in a rat model	15	8; F	Wistar (W)	N/A	4; C4-C5 to C7-C8	Open surgery, puncture with 23G needle	Started 1 week prior to insult	Systemic (oral administration)	Euthanized 5 months after puncture	MRI, histology
10.1016/j.spinee.2020.04.024	Deshmukh et al., 2020	A small-molecule inhibitor of the Wnt pathway, lorecivivint (SM04690), as a potential disease-modifying agent for the treatment of degenerative disc disease	18	10; no sex specified	SD	Ketamine-Xylazine	2; C8-C9, C9-C10	Digital palpation + fluoroscopy, percutaneous puncture with 20G needle	1 week	Intradiscal; 2 µL, no needle gauge specified	Euthanized 8 weeks after puncture	X-ray, histology
10.1002/jbm.b.34541	Hu et al., 2020	Thermosensitive hydrogels loaded with human-induced pluripotent stem cells overexpressing growth differentiation factor-5 ameliorate intervertebral disc degeneration in rats	24	300 g (~8-10 week); M	No details	Ketamine	3; C6-C7 to C8-C9	Fluoroscopy guided percutaneous puncture with 21G needle to depth of 5 mm w/ negative pressure (suction)	At the time of insult	Intradiscal; 2 µL, no needle gauge specified, cell delivery at 1x10^4/disc	Euthanized at 1, 2 and 3 months after transplantation	X-ray, MRI, histology
10.1152/ajpcell.00271.2019	He et al., 2020	P14ARF inhibits regional inflammation and vascularization in intervertebral disc degeneration by upregulating TIMP3	85	12; M	SD	Pentobarbital	1; C6-C7	Open surgery, puncture with 20G needle	1 week	Intradiscal, 2 µL through 33G needle	Euthanized 9 weeks after induction of degeneration	Histology, RT-qPCR, western blotting, IHC
10.2147/DDDT.S274812	Wang et al., 2020	Acacetin Alleviates Inflammation and Matrix degradation in Nucleus Pulposus Cells and Ameliorates Intervertebral Disc Degeneration in vivo	18	8; M	SD	Pentobarbital	2; level not specified	Digital palpation, percutaneous puncture with 21G to depth of 5 mm	Treatments delivered weekly	Systemic (IP delivery)	Euthanasia at 4 weeks after initial puncture	MRI, histology
10.1155/2020/8319516	Bi et al., 2020	Antiaging factor klotho retards the progress of intervertebral disc degeneration through the toll-like receptor 4-NF-kB pathway	12	12; M	SD	Pentobarbital	1; no details	Digital palpation + fluoroscopy, percutaneous puncture with 27G needle	siRNA delivered 1 day before IDD operation, and twice a week afterwards	Systemic (intravenous injection)	Euthanasia at 2 weeks after initial puncture	Histology, RT-PCR, western blotting
10.7150/THNO.47723	Zheng et al., 2021	A thermosensitive, reactive oxygen species-responsive MR409-encapsulated hydrogel ameliorates disc degeneration in rats by inhibiting the secretory autophagy pathway	10	12; F	SD	Pentobarbital	1; C7-C8	Fluoroscopy guided percutaneous puncture with 29G needle to depth of 2 mm	No treatment	No treatment	Euthanasia at 8 weeks after initial puncture	MRI, X-ray, histology, IHC

		The above paper had two separate animal models: one for induction of degeneration as outlined above, one for hydrogel delivery	50	12; F	SD	Pentobarbital	1; C7-C8	Fluoroscopy guided percutaneous puncture with 29G needle to depth of 2 mm	Treatment delivered at the time of insult	Intradiscal; 3 µL through 29G needle	Euthanasia at 8 and 12 weeks post puncture	X-ray, MRI, histology, IHC
10.1155/2020/6660429	Qin et al., 2020	Danshen attenuates intervertebral disc degeneration via antioxidation in SD rats	60	12; M + F	SD	Fluothane in oxygen/nitrous oxide	1; C8-C9	Digital palpation, percutaneous puncture with 20G through tail	Treatment delivered immediately following puncture	Systemic (oral administration)	Euthanasia 4 weeks after operation	X-ray, MRI, histology, biochemical analysis, IHC, western blotting
10.12998/wjcc.v8.i16.3431	Su et al. 2020	Application of molybdenum target X-ray photogrpahy in imaging analysis of caudal intervertebral disc degeneration in rats	21	10-12; M	SD	Chloral hydrate	1; C8-C9 or C9-C10	Digital palpation, percutaneous puncture with 18G needle	No treatment	No treatment	2-3 weeks	MRI, conventional X-ray, molybdenum target plain X-ray
10.1002/jsp2.1069	Chan et al. 2019	Pulsed electromagnetic fields reduce acute inflammation in the injured rat-tail intervertebral disc	72	12-16; F	SD	Isoflurane	3; C6-C7 to C8-C9	Fluoroscopy guided percutaneous puncture with 20G needle	Treatment started immediately following surgery	Treatment by exposure to pulsed electromagnetic field	4 or 7 days post insult	Histology, RT-PCR, ELISA
https://pubmed.ncbi.nlm.nih.gov/31337166/	Qian et al., 2019	Selection of the optimal puncture needle for induction of a rat intervertebral disc degeneration model	24	12; M	SD	Chloral hydrate	3; C7-C8 to C9-C10	Fluoroscopy guided percutaneous puncture with 16, 18, or 26G needles	No treatment	No treatment	Sacrificed at 1, 2, or 4 weeks post-insult	MRI, histology, IHC
10.1007/s00586-019-05924-3	Li et al., 2019	Diffusion kurtosis imaging provides quantitative assessment of the microstructure changes of disc degeneration: an in vivo experimental study	21	12; F	SD	N/A	1; C6-C7 or C7-C8	Fluoroscopy guided percutaneous puncture with 21G needle to depth of 5 mm	No treatment	No treatment	Up to 14 days	MRI (diffusion weighted and diffussion kurtosis imaging), histology
10.1016/j.jos.2018.08.006	Zhang et al., 2019	Effect of hyperlipidaemia to accelerate intervertebral disc degeneration in the injured rat caudal disc model	30	8-10; M	W	N/A	1; C7-C8	Open surgery, puncture with 20G needle	Diet modified 8-weeks prior to surgery	Systemic (dietary changes)	8 weeks from puncture	Histology, IHC, western blotting, RT-qPCR
10.1155/2019/7189854	Liu et al., 2019	Aspirin-mediated attenuation of intervertebral disc degeneration by ameliorating reactive oxygen species in vivo and in vitro	40	12; M	SD	Pentobarbital	2; C8-C9, C9-C10	Digital palpation + fluoroscopy guided percutaneous puncture with 20G needle to depth of 5 mm	3 days post puncture	Intradiscal; 2 µL through 33G	7 days following insult	X-ray, MRI, histology, IHC
10.1186/s13075-019-1986-8	Zhan et al., 2019	Long non-coding RNA HOTAIR modulates intervertebral disc degenerative changes via Wnt/B-catenin pathway	10	12; M	SD	Ketamine/ketamine hydrochloride	3; C6-C7 to C8-C9	Digital palpation + fluoroscopy guided percutaneous puncture with 21G needle	At the time of insult	Intradiscal; 2 µL through 31G	Euthanasia 4 weeks after puncture	X-ray, MRI, histology
10.1016/j.intimp.2018.10.024	Fang et al., 2018	Wogonin mitigates intervertebral disc degeneration through the Nrf2/ARE and MAPK signaling pathways	48	150 g (~6 week); M	SD	Pentobarbital	1; C7-C8 or C8-C9	Fluoroscopy guided percutaneous puncture with 20G needle to depth of 5 mm	At the time of insult and repeated weekly	Intradiscal; 2 µL through 31G	8 weeks after initial injection	MRI, histology
10.1038/s41598-018-35011-4	Matta et al., 2018	NTG-101: A Novel Molecular Therapy that Halts the Progression of Degenerative Disc Disease	27	12; F	W	N/A	5; no details	Fluoroscopy guided percutaneous puncture with 27G	4 weeks	Intradiscal; 8 µL through 32G	10 weeks post insult	Histology, IHC
10.1016/j.actbio.2018.07.008	Moriguchi et al., 2018	In vivo annular repair using high-density collagen gel seeded with annulus fibrosus cells	42	10-12; M	Athymic nude (AN)	N/A	1; C3-C4	Open surgery, puncture with 18G needle	At the time of insult	Focus on annular repair model	2 weeks and 5 weeks	MRI, X-ray, histology
10.1016/j.jot.2018.07.008	Ni Li et al., 2018	Disc degeneration promotes regional inhomogeneity in the trabecular morphology of loaded rat tail vertebrae	30	12; M	SD	Pentobarbital	2; C8-C9, C9-C10	Digital palpation percutaneous puncture with 18G needle	No treatment	No treatment	1 week	X-ray, MRI, histology
10.12659/MSM.910636	Chen et al., 2018	Time-course investigation of intervertebral disc degeneration induced by different sizes of needle punctures in rat tail disc	36	16-24; no sex specified	SD	Chloral hydrate and isoflurane	3; C5-C6, C7-C8, C9-C10	Fluoroscopy guided percutaneous puncture with 18, 21, or 25G needle	No treatment	No treatment	2, 4 and 6 weeks	X-ray, MRI, histology, RT-PCR
10.1038/s41419-017-0151-z	Wu X et., 2018	Prolactin inhibits the progression of intervertebral disc degeneration through inactivation of the NF-κB pathway in rats article	80	12; M	SD	Chloral hydrate	2; C7-C8, C8-C9	Digital palpation percutaneous puncture with 20G needle	At the time of insult	Intradiscal; 2 µL through 33G	4,7,14,28 days	X-ray, MRI, histology, IHC

10.1002/jor.23628	Hu et al., 2018	Optimization of puncture injury to rat caudal disc for mimicking early degeneration of intervertebral disc	Stage 1: 12; Stage 2: 30	12; no sex specified	W	Pentobarbital	Stage 1: 6, no details; Stage 2: 3, C6-C7 to C8-C9	Digital palpation + fluoroscopy guided percutaneous puncture with 18, 21, 23, 25, 27, or 29G needle	No treatment	No treatment	2, 4, 6, 8 weeks post insult	X-ray, MRI, histology, IHC, RT-qPCR
10.7150/ijbs.24081	Chen et al., 2018	Berberine suppresses apoptosis and extracellular matrix (ECM) degradation in nucleus pulposus cells and ameliorates disc degeneration in a rodent model	48	8; M	SD	Chloral hydrate	1; C7-C8	Digital palpation + fluoroscopy guided percutaneous puncture with 27G to depth of 4 mm	Immediately after insult	Systemic (intragastric)	0, 4, 8 weeks post insult	MRI, histology, IHC
10.22603/ssrr.2017-0026	Sato et al., 2018	Vascular endothelial growth factor in degenerating intervertebral discs of rat caudal vertebrae	48	250-300 g (~8-10 week); M	SD	Pentobarbital	3; C5-C6 to C7-C8	Open surgery, punctured with 26G needle to a depth of 2 mm 10 times	No treatment	No treatment	1, 7, 14, 28 days	Histoloy, ELISA, IHC
10.3389/fphar.2018.01043	Liu et al, 2018	Urolithin A Inhibits the Catabolic Effect of TNFα on Nucleus Pulposus Cell and Alleviates Intervertebral Disc Degeneration in vivo	30	12; M	SD	Pentobarbital	2; C7-C8, C8-C9	Digital palpation, percutaneous puncture with 21G needle to depth of 5 mm	One day	Systemic (dietary supplement)	4 weeks	X-ray, MRI, histology
10.1038/s41598-017-17289-y	Makino et al., 2017	A selective inhibition of c-Fos/activator protein-1 as a potential therapeutic target for intervertebral disc degeneration and associated pain	32	12; no sex specified	SD	Medetomidine, midazolam, and butorphanol tartrate	2; C6-C7, C7-C8	Digital palpation, percutaneous puncture with 20G needle either to depth of 5 mm, or through entire tail	One day	Systemic (dietary supplement)	4, 8 weeks	X-ray, MRI, histology, IHC, tail-flick latency
10.1016/j.otsr.2017.04.005	Zamora et al., 2017	Effect of Propionibacterium acnes (PA) injection on intervertebral disc degeneration in a rat model: Does it mimic modic changes?	12	400-500 g (~10-14 week); M	SD	Isoflurane	1; C4-C5	Digital palpation, percutaneous puncture with 18G needle to depth of 5 mm	At the time of insult	Intradiscal; 5 µL through 18G	12 Weeks	MRI, histology
10.1007/s00586-016-4898-1	Wang et al., 2017	Repairing the ruptured annular fibrosus by using type I collagen combined with citric acid, EDC and NHS: an in vivo study	48	5-6; M	SD	Pelltobarbitalum natricum	1; C3-C4	Open surgery, puncture with 18G needle	At the time of insult	Focus on annular repair model	4 weeks	X-ray, MRI, histology
10.1016/j.phrs.2017.01.005	Xu et al., 2017	Hydrogen sulfide protects against endoplasmic reticulum stress and mitochondrial injury in nucleus pulposus cells and ameliorates intervertebral disc degeneration	48	12; M	SD	Pentobarbital	1; C7-C8	Digital palpation, percutaneous puncture with 20G needle to depth of 4 mm	Immediately after insult	Systemic (IP delivery)	4 and 8 weeks	MRI, histology
10.1002/jor.23114	Cunha et al., 2017	Joint analysis of IVD herniation and degeneration by rat caudal needle puncture model	14	10; M	W	Isoflurane	3; C5-C6 to C7-C8	Fluoroscopy guided percutaneous puncture with 21 or 25G needle to depth of 5 mm	No treatment	No treatment	2, 6 weeks	X-ray, histology, IHC, biochemical analysis
10.1002/jor.23350	Maidhof et al., 2017	Timing of mesenchymal stem cell delivery impacts the fate and therapeutic potential in intervertebral disc repair	46	350-400 g (~10-12 week); M	SD	N/A	3; C4-C5 to C6-C7	Open surgery, puncture with 27G to depth of 4 mm	3, 14, or 30 days post injury	Open surgery; intradiscal delivery of 5 µL through 33G, cells at 5x10^3/disc	0, 1, 7, or 14 days post treatment	Histology, biomechanic analysis, biochemical analysis
10.18632/oncotarget.14389	Li et al., 2017	Epoxyeicosanoids prevent intervertebral disc degeneration in vitro and in vivo	40	12; M	SD	Diethyl ether	1; C5-C6 to C7-C8	Fluoroscopy guided percutaneous puncture with 21G needle to depth of 5 mm	At the time of insult; 9 more doses given over the next 15 days	Percutaneous puncture; Intradiscal delivery of 2 µL through 31G	4 weeks	X-ray, MRI, histology
10.1007/s12640-016-9676-7	Castania et al., 2017	The Presence of the Neuronal Nitric Oxide Synthase Isoform in the Intervertebral Disk	40	10; M	W	Ketamine-Xylazine	3; C6-C7 to C8-C9	Digital palpation + fluoroscopy guided percutaneous puncture with 21G needle until tactile resistance from contralateral AF was observed	Immediately after insult	Percutaneous puncture; intradiscal delivery of 2 µL through 30G	2 or 21 days	MRI, histology, RT-qPCR, IHC
10.1016/j.yexcr.2017.08.011	Liu et al., 2017	MicroRNA-132 upregulation promotes matrix degradation in intervertebral disc degeneration	60	12; no sex specified	SD	Ketamine-Xylazine	1; C6-C7	Open surgery, puncture with 31G needle to depth of 1.5 mm	At the time of insult	Open surgery; intradiscal delivery through 31G, no volume stated	4 weeks	IHC, RT-qPCR, western blotting
10.1117/12.2255761	Horne et al., 2017	Low intensity pulsed ultrasound (LIPUS) for the treatment of intervertebral disc degeneration	5	12; F	SD	N/A	3; no details	Fluoroscopy guided percutaneous puncture with 20G needle until contralateral AF was reached	30 minutes following insult, and daily for 5 days	Systemic (ultrasound exposure)	5 days	Histology, RT-qPCR
	Hua et al., 2016	The relationship between MRI and histology in a rat model of intervertebral disc degeneration	44	12; M	SD	Pentobarbital	2; C7-C8, C8-C9	Digital palpation guided percutaneous puncture with 20G needle to depth of 5 mm	No treatment	No treatment	4, 8, 12, 24 weeks post-surgery	MRI, histology

10.1007/s10735-015-9651-2	Zhang et al., 2016	Production of CCL20 on nucleus pulposus cells recruits IL-17-producing cells to degenerated IVD tissues in rat models	40	8-10; M	W	Pentobarbital	1; C6-C7	Open surgery, puncture with 20G needle to depth of 5 mm	No treatment for caudal model	No treatment for caudal model	5 weeks	IHC, RT-PCR, western blotting, ELISA
10.3390/ijms17020147	Liao et al., 2016	Cell therapy using bone marrow-derived stem cell overexpressing BMP-7 for degenerative discs in a rat tail disc model	Stage 1: 12; Stage 2: 60	8; M	Lewis (L)	Isoflurane	2; C6-C7, C8-C9	Fluoroscopy guided percutaneous puncture with 18 or 22G needle.	At time of insult, 2 weeks, or 4 weeks after insult	Intradiscal; no needle gauge discussed for treatment delivery; cells delivered at 1x10^4/disc	8 Weeks	X-ray, histology
10.1590/1413-78522016240115296O	De Campos et al., 2016	Studies of molecular changes in intervertebral disc degeneration in animal model	12	12; M	W	Ketamine-Xylazine	3; C6-C7 to C8-C9	Fluoroscopy guided percutaneous puncture with 20G needle	No treatment	No treatment	15 or 28 days post puncture	Histology, IHC, RT-PCR
10.1016/j.biomaterials.2015.02.024	Feng et al., 2015	Gene therapy for nucleus pulposus regeneration by heme oxygenase-1 plasmid DNA carried by mixed polyplex micelles with thermo-responsive heterogeneous coronas	32	12; no sex specified	SD	Isoflurane	2; C5-C6, C7-C8	Open surgery puncture with 21G needle to depth of 5 mm	2 weeks	Fluoroscopy guided percutaneous puncture; intradiscal delivery of 2 µL through 31G	6 weeks after initial puncture (4 weeks after treatment)	X-ray, histology, IHC
10.1590/S0102-86502015008000009	Issy et al., 2015	Does a small size needle puncture cause intervertebral disc changes	14	300-350 g (~8-10 week); M	W	Ketamine-Xylazine	3; C7-C8 to C9-C10	Digital palpation + fluoroscopy guided percutaneous puncture with 21G needle	At the time of puncture	Percutaneous intradiscal delivery of 2 µL through 30G	2, 15, 42 days	MRI, Histology
10.1097/BSD.0000000000000141	Inoue et al., 2015	The effect of bone morphogenetic protein-2 injection at different time points on intervertebral disk degeneration in a rat tail model	25	12; M	L	Isoflurane	2; C7-C8, C8-C9	Digital palpation + fluoroscopy guided percutaneous puncture with 18G needle to depth of 5 mm	4, 6, 8 weeks post puncture	Digital palpation percutaneous puncture; intradiscal delivery of 5 µL through 27G	6 weeks post treatment	X-ray, MRI, histology, IHC
10.1016/j.actbio.2015.06.006	Grunert et al., 2015	Riboflavin crosslinked high-density collagen gel for the repair of annular defects in intervertebral discs: An in vivo study	35	10-12; no sex specified	AN	N/A	1; C3-C4	Open surgery, puncture with 18G needle	At time of insult	Focus on annular repair model	5 and 18 weeks	MRI, histology, mechanical testing
10.1371/journal.pone.0113161	Silveira et al., 2014	Protective effects of cannabidiol on lesion-induced intervertebral disc degeneration	19	300-350 g (~8-10 week); M	W	Ketamine-Xylazine	2; C6-C7, C8-C9	Digital palpation guided percutaneous puncture with 21G needle to contralateral AF	At time of insult	Intradiscal; 2 µL through 30G	15 days after the disc puncture	MRI, histology
10.1016/j.spinee.2014.03.050	Ming-Hsiao et al., 2014	Lovastatin prevents discography-associated degeneration and maintains the functional morphology of intervertebral discs	12	12; no sex specified	W	N/A	6; no details	Fluoroscopy guided percutaneous puncture with 27G needle	At time of insult	Intradiscal; 50 µL through 27G	2 or 4 weeks	Histology, IHC, RT-qPCR
10.1016/j.spinee.2013.11.034	Than et al., 2014	Intradiscal injection of simvastatin results in radiologic, histologic, and genetic evidence of disc regeneration in a rat model of degenerative disc disease	272	12; no sex specified	SD	Isoflurane	2; C5-C6, C7-C8	Digital palpation + fluoroscopy guided percutaneous puncture with 21G needle to depth of 5 mm	6 weeks post insult	Percutaneous intradiscal delivery of 2 µL through 31G	2, 4, 8, 12, and 24 weeks post treatment	MRI, histology, RT-PCR
10.1097/BRS.0000000000000194	Grunert et al., 2014	Assessment of intervertebral disc degeneration based on quantitative magnetic resonance imaging analysis: An in vivo study	24	190-250 g (~8-10 week); M	AN	Isoflurane	1; C3-C4	Independent sets testing open surgery and percutaneous punctures, both with 18G needle	At time of insult	Focus on annular repair model	1 and 3 months	MRI, histology
10.1097/BRS.0000000000000103	Grunert et al., 2014	Annular repair using high-density collagen gel: A rat-tail in vivo model	42	10-12; M	AN	N/A	1; C3-C4	Open surgery, puncture with 18G needle	At time of insult	Focus on annular repair model	5 weeks	MRI, X-ray, histology
10.1177/0885328213515034	Yan et al., 2014	Effects of releasing recombinant human growth and differentiation factor-5 from poly(lactic-co-glycolic acid) microspheres for repair of the rat degenerated intervertebral disc	N/A	12; M	SD	Chloral hydrate	3; C4-C5, C5-C6, C7-C8	Open surgery, puncture with 21G needle	4 weeks post insult	Intradiscal; unknown volume, through 31G	8 weeks post treatment	X-ray, MRI, histology, biochemical analysis, RT-qPCR
10.1016/j.actbio.2013.08.019	Liang et al., 2013	Dual release of dexamethasone and TGF-β3 from polymeric microspheres for stem cell matrix accumulation in a rat disc degeneration model	96	12; M	SD	Pentobarbital	2; C7-C8, C8-C9	Digital palpation percutaneous puncture with 20G needle to depth of 5 mm	2 weeks post injury	Intradiscal; 2 µL through 31G, cells at 1x10^6 cells/mL	4, 8, 16, 24 weeks post treatment	X-ray, MRI, histology, IHC, biochemical analysis, RT-qPCR

10.3892/mmr.2013.1450	Zou et al., 2013	Efficacy of intradiscal hepatocyte growth factor injection for the treatment of intervertebral disc degeneration	30	200-250 g (~6-8 week); M	SD	Ketamine-Xylazine	2; C5-C6, C7-C8	Fluoroscopy guided percutaneous puncture with 21G needle	4 weeks post insult	Intradiscal delivery; 2 µL through 31G	2 or 4 weeks post treatment	MRI, histology, IHC
10.1186/ar4224	Rastogi et al., 2013	MMP-2 mediates local degradation and remodeling of collagen by annulus fibrosus cells of the intervertebral disc	N/A	26-32; no sex specified	SD	Isoflurane	1; C6-C7	Open surgery with fluoroscopy to confirm appropriate depth; puncture with either 26G, 22G, or 18G	No in vivo treatment	No in vivo treatment	2 weeks	Histology, IHC
10.1590/1414-431X20122429	Issy et al., 2013	Experimental model of intervertebral disc degeneration by needle puncture in Wistar rats	16	300-350 g (~8-10 week); M	W	Ketamine-Xylazine	2; C6-C7, C8-C9	Digital palpation + fluoroscopy guided puncture with 20G needle, until resistance from contralateral AF was observed	No treatment	No treatment	7 or 30 days post puncture	X-ray, MRI, histology
10.1016/j.spinee.2013.01.040	Tsai et al., 2013	Increased periostin gene expression in degenerative intervertebral disc cells	8	8; M	L	N/A	2; C6-C7, C8-C9	Digital palpation + fluoroscopy guided puncture with 18G needle	No treatment	No treatment	8 weeks post puncture	Histology, IHC
10.1590/S1413-78522013000300003	Oliveira et al., 2013	Extracellular matrix remodeling in experimental intervertebral disc degeneration	3	12; M	W	Ketamine-Xylazine	2; C6-C7, C8-C9	Digital palpation, percutaneous puncture with 20G needle	No treatment	No treatment	0, 15, 30 days	IHC
10.3171/2011.5.SPINE10811	Zhang et al., 2011	Time course investigation of intervertebral disc degeneration produced by needle-stab injury of the rat caudal spine: Laboratory investigation	32	12; M	SD	Isoflurane	2; C5-C6, C7-C8	Fluoroscopy guided percutaneous puncture with 21G needle to depth of 5 mm	No treatment	No treatment	3, 10, 17, 42 days	MRI, histology, RT-qPCR, biochemical analysis
10.1016/j.spinee.2010.08.013	Keorochana et al, 2010	The effect of needle size inducing degeneration in the rat caudal disc: Evaluation using radiograph, magnetic resonance imaging, histology, and immunohistochemistry	36	12-14; M	L	Isoflurane	2; C6-C7, C8-C9	Digital palpation + fluoroscopy guided percutaneous puncture with 18, 20, or 22G needle to depth of 5 mm	No treatment	No treatment	2, 4, 6, 8 weeks	X-ray, MRI, histology, IHC
10.1186/ar2861	Zhang et al., 2009	Intradiscal injection of simvastatin retards progression of intervertebral disc degeneration induced by stab injury	30	12; no sex specified	SD	Isoflurane	2; C5-C6, C7-C8	Open surgery using fluoroscopy to guide puncture depth; puncture using 21G needle to depth of 5 mm	4 weeks post insult	Intradiscal delivery of 2 µL through 31G	2 weeks post treatment	MRI, histology, biochemical analysis, RT-qPCR
10.3171/2009.4.SPINE08744	Zhang et al., 2009	The effects of punctured nucleus pulposus on lumbar radicular pain in rats: A behavioral and immunohistochemical study - Laboratory investigation	72	200-250 g (~6-8 week); M	SD	Pentobarbital	2; C4-C5, C8-C9	Open surgery, puncture with 21G needle to depth of 3 mm	No treatment on caudal model	No treatment on caudal model	2 weeks	MRI, histology
10.3171/2009.2.SPINE08925	Zhang et al., 2009	Developing consistently reproducible intervertebral disc degeneration at rat caudal spine by using needle puncture - Laboratory investigation	9	12; M	SD	Isoflurane	2; C5-C6, C7-C8	Open surgery + fluoroscopy guided puncture with 18G or 21G to depth of 5 mm	No treatment	No treatment	3 months	MRI, histology, IHC
10.1097/BRS.0b013e31819c09c4	Hsieh et al., 2009	Degenerative anular changes induced by puncture are associated with insufficiency of disc biomechanical function	36	32-36; no sex specified	SD	Isoflurane	1; C6-C7	Fluoroscopy guided percutaneous puncture with 18, 22, or 26G needle to depth of 2 mm	No treatment	No treatment	1, 2, 4 weeks	Histology; mechanical testing done in parallel in organ culture model
10.1097/BRS.0b013e31817c64a9	Han et al., 2008	A simple disc degeneration model induced by percutaneous needle puncture in the rat tail	163	12; M	SD	Chloral hydrate	2; C7-C8, C8-C9	Digital palpation + fluoroscopy guided percutaneous puncture with 20G needle either to depth of 5 mm or through contralateral aspect of tail	No treatment	No treatment	1, 2, 4 weeks	X-ray, histology, biochemical analysis
10.1097/BRS.0b013e31815b9850	Ulrich et al. 2007	Repeated disc injury causes persistent inflammation	48	12; sex not specified	SD	Ketamine-Xylazine	3; C5-C6 to C7-C8	Open surgery and disc stab with number 11 blade, then fluoroscopy guided percutaneous puncture with 23G needle to depth of 1.5 mm (either single stab or triple stab)	No treatment	No treatment	Single-stab discs were examined 4, 7, 14, 28, and 56 days. Triple-stab discs were examined 9, 14, 28, and 56 days	Histology, ELISA, IHC
10.1097/01.brs.0000251013.07656.45	Rousseau et al., 2007	Stab Incision for Inducing Intervertebral Disc Degeneration in the Rat	24	12; sex not specified	SD	Ketamine-Xylazine	3; C5-C6 to C7-C8	Open surgery, stab with number 11 blade to depth of 1.5 mm	No treatment	No treatment	4, 7, 14, 28 days	Histology, ELISA, ex vivo mechanical testing
10.1080/15476286.2021.1898176	Wang et al. 2021	MicroRNA-140-3p alleviates intervertebral disc degeneration via KLF5/N-cadherin/MDM2/Slug axis	64	12; M	SD	Chloral hydrate	1; C7-C8	Fluoroscopy guided percutaneous puncture with 21G needle	Immediately	Intradiscal delivery of treatment; no volume or needle gauge reported	4, 7, 14, 28 days post puncture	X-ray, histology, RT-qPCR

10.3389/fcell.2021.687024	Liu et al. 2021	Fexofenadine protects against intervertebral disc degeneration through TNF signaling	18	8-12; M	SD	N/A	1; C8-C9	Digital palpation, percutaneous puncture with 20G needle to depth of 5 mm	Every other day	Systemic (intraperitoneal) treatment delivery	7 days	Histology, RT-PCR, western blotting, ELISA, IHC
10.1016/j.lfs.2021.119874	Wang et al. 2021	17Beta-estradiol alleviates intervertebral disc degeneration by inhibiing NF-kB signal pathway	18	12; F	SD	N/A	1; C6-C7	Digital palpation guided percutaneous puncture with 21G needle to depth of 3 mm	3 days post insult	Systemic (subcutaneous treatment delivery)	8 weeks	X-ray, MRI, histology, IHC
10.1155/2021/6632786	Yu et al. 2021	Mangiferin alleviates mitochondrial ROS in nucleus pulposus cells and protects against intervertebral disc degeneration via suppression o fNF-kB signaling pathway	15	12; no sex specified	SD	Pentobarbital	2; C8-C9, C9-C10	Digital palpation + fluoroscopy guided percutaneous puncture with 20G needle to depth of 5 mm	3 days post insult	Intradiscal; 2 µL through 33G	7 days after initial puncture, 4 days after treatment	X-ray, MRI, histology, IHC
10.3390/ijms222111355	Kim et al. 2021	Activation of hypoxia-inducible factor-1alpha signaling pathway has the protective effect of intervertebral disc degeneration	10	8; M	SD	Isoflurane	4; C4-C5 to C7-C8	Fluoroscopy guided percutaneous puncture with 21G needle	At time of insult	Intradiscal delivery of unknown volume through 21G needle	8 weeks	X-ray, MRI, histology, IHC
10.1007/s10495-022-01707-2	Wu et al. 2022	SKI knockdown suppresses apoptosis and extracellular matrix degradation of nucleus pulposus cells via inhibition of the Wnt/β-catenin pathway and ameliorates disc degeneration	40	200-230 g (~6-8 week); M	SD	Pentobarbital	1; C7-C8	Digital palpation guided percutaneous puncture with 21G needle	At time of insult	Intradiscal delivery of 2 µL through 21G	8 weeks	Histology, MRI, RT-qPCR, western blotting, IHC
10.1038/s12276-022-00729-9	Zhang et al. 2022	Cytosolic escape of mitochondrial DNA triggers cGAS-STING-NLRP3 axis-dependent nucleus pulposus cell pyroptosis	7	12; sex not specified	SD	Pentobarbital	2; C8-C9, C9-C10	Digital palpation guided percutaneous puncture with 29G needle to depth of 5 mm	At time of insult and repeated weekly for 1 month	Intradiscal percutaneous delivery of 2 µL through 29G	1 month	X-ray, MRI, histology, IHC
10.1186/s10020-021-00351-x	Cheng et al. 2021	CB2-mediated attenuation of nucleus pulposus degeneration via the amelioration of inflammation and oxidative stress in vivo and in vitro	40	400 g (~10-14 week); M	SD	Chloral hydrate	1; C7-C8	Fluoroscopy guided percutaneous puncture with 21G needle	Weekly	Open surgery, intradiscal delivery of 2 µL, no needle gauge stated for treatment delivery	1, 2, 3, 4 weeks	X-ray, MRI, histology, IHC
10.1038/s41598-021-94173-w	Matta et al. 2021	A comparative study of mesenchymal stem cell transplantation and NTG-101 molecular therapy to treat degenerative disc disease	30	12; F	W	Isoflurane	5; no details	Fluoroscopy guided percutaneous puncture with 26G needle through contralateral AF	10 weeks post injury	Percutaneous intradiscal delivery of 8 µL through 32G; cells at 150,000 cells/disc	10 weeks post treatment	Histology, IHC, western blotting, RT-qPCR